

Periodic Microwave Spikes from a Magnetic-Field-Free Hollow-Cathode Discharge

D. Arbel, Z. Bar-Lev, J. Felsteiner, A. Rosenberg, and Ya. Z. Slutsker

Physics Department, Technion-Israel Institute of Technology, 32000 Haifa, Israel

(Received 30 May 1996)

Periodic nanosecond pulses of microwave radiation were observed from a low-pressure magnetic-field-free hollow-cathode discharge. These microwave spikes were emitted when the discharge current exceeded the threshold for the periodic collapse of the cathode sheath, each collapse cycle corresponding to one spike. The spikes were found to appear at the same phase of the collapse cycle. The peak power of each spike was about 10 W. A wide frequency spectrum was observed above the electron plasma frequency of the discharge plasma, ranging from a few GHz up to at least 20 GHz. [S0031-9007(96)02029-7]

PACS numbers: 52.80.Hc

We have observed periodic nanosecond pulses of microwave radiation generated in a magnetic-field-free hollow-cathode discharge. These microwave spikes have been found to accompany the previously reported [1] strong rf discharge-current oscillations which follow the periodic collapse of the cathode sheath. We have also found that each microwave spike appears together with a spike of plasma waves near the cathode. Both of these spikes appear at a certain phase of the discharge-current oscillation. We present here experimental results supporting the following physical process: Above a certain discharge current the cathode sheath collapses, namely, the sheath voltage rapidly falls down to electron temperature level [1]. Then the sheath voltage is reconstructed, creating a beam of electrons emitted from the cathode into the discharge plasma. This beam, in turn, causes a beam-plasma instability. This instability leads to the generation of plasma waves and microwave radiation till the next cathode-sheath collapse. Typically the complete cycle is few tens of ns long, whereas the microwave pulses are shorter than about one quarter of this period.

The known phenomena of electromagnetic-wave generation in hollow-cathode discharge devices are related to charged particles orbiting either in a strong external magnetic field [2] or around a thin wire located along the hollow-cathode axis and acting as an anode [3]. To the contrary, in our experiments no external magnetic field and no wire anode were applied but significant microwave radiation was unexpectedly obtained from this very simple device.

The experimental apparatus is shown in Fig. 1. We used a discharge tube composed of an open-ended cylindrical cathode, 10 cm long, having an inside diameter of 8.6 cm. The anode was located close to one end of the cathode. These electrodes were mounted inside a glass vessel filled with He. Changing of the anode shape, diameter, location, or material had no influence on the experimental results. Similar results, with no qualitative differences, were obtained with a cathode diameter of 4.1 cm or with Ne or Ar instead of He. Typical operating

pressures P were between 50 and 500 mTorr. The discharge was driven by a pulse generator with a pulse duration of $2 \mu\text{s}$. Typical discharge currents I_a were between 5 and 120 A with the tube voltage V_c varied correspondingly between 350 and 800 V. This voltage was very close to the discharge cathode fall. The electron temperature and spatial distribution of the plasma density were measured by movable and surface probes. The plasma density n_e was found to be directly proportional to the discharge current I_a anywhere within the cylinder. For example, we obtained $n_e \approx 8 \times 10^{10} I_a \text{ cm}^{-3}$ at the cathode axis, $n_e \approx 3 \times 10^{10} I_a \text{ cm}^{-3}$ at 0.3 cm from the cathode wall, and $n_e \approx 1 \times 10^{10} I_a \text{ cm}^{-3}$ near the cathode-sheath edge. The full two-dimensional spatial distribution of the plasma density inside the hollow cathode is shown in Fig. 2. The density inhomogeneity is seen here clearly. The bulk plasma electrons were found to have a Maxwellian distribution with temperature T_e around 7–8 eV. An electrostatic multigrad plasma analyzer located at the cathode surface was used to investigate the high-energy part in the electron distribution function of the discharge plasma. For more apparatus details see Ref. [1].

The microwaves radiated from the hollow cathode were received by either half-wave dipoles or open-ended waveguides or microwave horns located outside the vacuum vessel. These antennas were connected directly

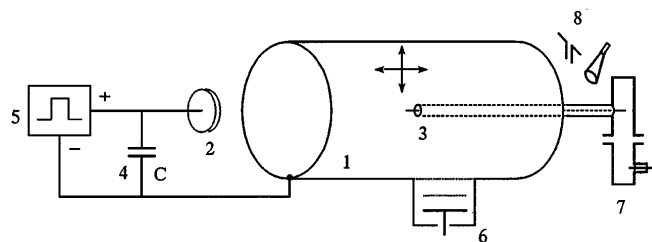


FIG. 1. Experimental apparatus. 1—cathode cylinder; 2— anode; 3—movable plasma-wave antenna; 4—shunt capacitor; 5—pulse generator; 6—electrostatic plasma analyzer; 7— microwave filter; 8—microwave antennas.

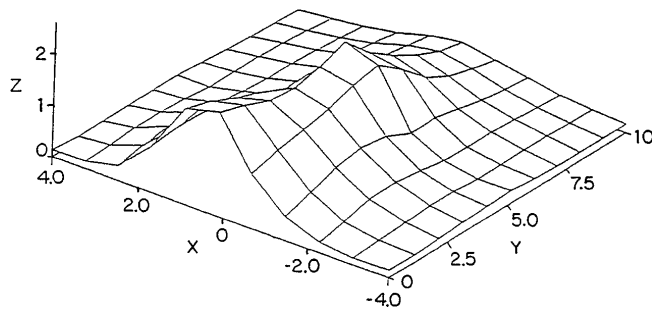


FIG. 2. Spatial distribution of the plasma density. x —radial distance from the cylinder axis in cm. y —distance from the open end (anode side) of the cylinder in cm. z —plasma density (arbitrary units).

to microwave diodes or to a spectrum analyzer. Plasma waves excited in the discharge plasma were investigated by a small movable coaxial open-ended antenna (see Fig. 1). Its total diameter was 2 mm, and its sensing end had a diameter of 0.7 mm and a length of 1.5 mm. This antenna was connected to a microwave diode or to a spectrum analyzer via a high-pass microwave filter.

Microwave radiation from the discharge plasma appeared only in the state of periodic collapse of the cathode sheath. In this case strong oscillations in the discharge current with a frequency of about a few tens of MHz appeared during the $2\text{-}\mu\text{s}$ current pulse [1]. This frequency is close to the ion plasma frequency near the cathode sheath. The scope trace of the detected signal from the microwave antenna is shown in Fig. 3 (top). The signal coming from the plasma-wave antenna had exactly the same shape; therefore, it is not shown here. The discharge current trace is shown in Fig. 3 (bottom). One can clearly see that the current oscillations and the microwave spikes have the same repetition rate and a constant phase shift between them. The radiation coming out from each open end of the cathode cylinder was found to be unpolarized and isotropic with a wide noiselike spectrum. An example of this spectrum is shown in Fig. 4. The frequency spectrum of the plasma waves had approximately the same range and a similar shape. The two-dimensional spatial distribution of the plasma-wave intensity is shown in Fig. 5. Its shape was found to be independent of the discharge current. It is clearly

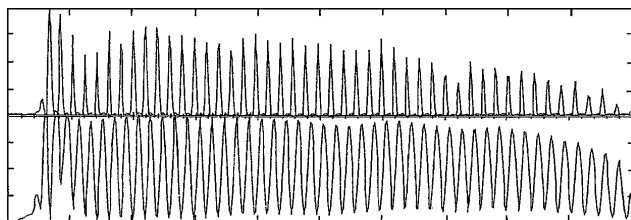


FIG. 3. Scope traces of the microwave intensity (top) and the discharge current oscillations (bottom). Time base 200 ns/div; $I_a = 15$ A; $P = 0.1$ Torr. Vertical scale in arbitrary units.

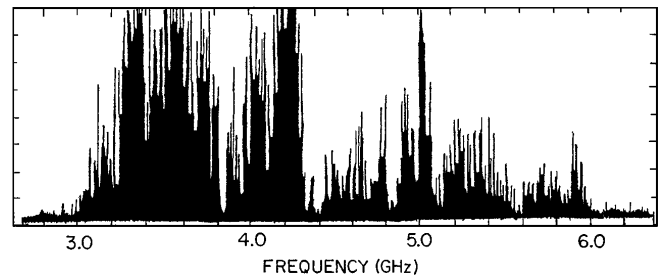


FIG. 4. Spectrum of the microwave intensity (linear scale, arbitrary units). $I_a = 15$ A; $P = 0.1$ Torr.

seen that the plasma waves are mainly concentrated in a region of about 0.3–0.5 cm near the cathode wall (here $n_e \approx 3 \times 10^{10} I_a \text{ cm}^{-3}$). Taking into account the sensitivity of plasma-wave antennas [4] we estimated the maximal measured electric field in the electron plasma oscillations to be 500–1000 V/cm. As it is seen from the spectrum in Fig. 4 the minimum radiated frequency, $f_{\min} \approx 3$ GHz, detected for $I_a = 15$ A was close to the electron plasma frequency $\omega_e/2\pi$ near the cathode-sheath edge where $n_e \approx 1 \times 10^{10} I_a \text{ cm}^{-3}$. The maximum spectrum intensity of the radiated microwaves appeared at a frequency which corresponded to the value of $\omega_e/2\pi$ at a distance 0.3–0.5 cm from the wall. The maximum radiated frequency f_{\max} was approximately 6 GHz, i.e. $f_{\max} \approx 2f_{\min}$. This approximate relation was found to hold for all the investigated current range (for the higher currents the spectrum is just a bit wider).

The intensity of both the radiated microwaves and the plasma waves have been found to increase monotonically with the discharge current [see Fig. 6(a)]. The threshold discharge currents for the creation of the microwaves and the plasma waves have been found to be quite close: 8 and 9 A. This small difference can be explained by the fact that the microwave antenna receives the radiation from all the plasma volume while the plasma-wave antenna is sensitive mainly locally. The peak power of each microwave spike reached ~ 10 W at a discharge current of 40 A. It should be noted that the current needed for the periodic collapse of the cathode sheath, i.e., for the appearance of the strong discharge current oscillations, is

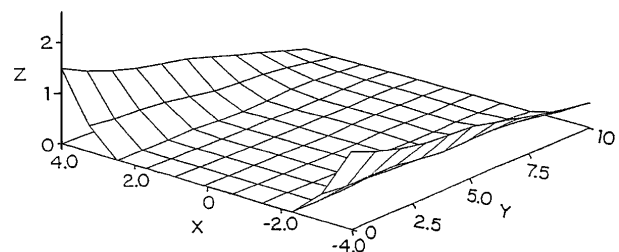


FIG. 5. Spatial distribution of the plasma-wave intensity. x and y —same as in the caption for Fig. 2. z —plasma-wave intensity (arbitrary units).

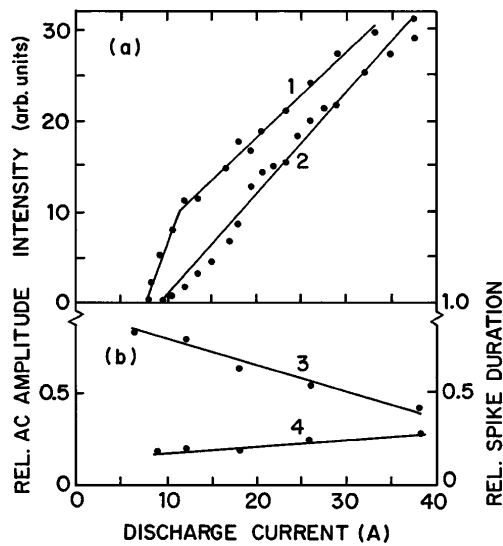


FIG. 6. (a) The microwave (1) and plasma-wave (2) intensities vs the discharge current I_a . (b) The relative ac amplitude (3) and the relative spike duration (4) vs the discharge current I_a . $P = 0.1$ Torr.

a bit smaller: between 5 and 6 A. Contrary to the trend of the microwave intensity, the relative ac amplitude I_{ac}/I_a of the current oscillations decreases with the growth of the dc discharge current I_a [see Fig. 6(b)]. Here I_{ac} is the oscillating part of the discharge current. The ratio of the full spike duration at half maximum of a spike to the repetition period of the spikes is also shown in Fig. 6(b) as a function of the discharge current. It is seen that this ratio becomes larger with the discharge current. In Fig. 7 we show the microwave intensity and the corresponding relative ac amplitude of the discharge current vs the pressure P for two different values of the discharge current (20 and 42 A). It is seen that when P is increased the microwave intensity decreases significantly while there is only a small decrease in the relative ac current amplitude. To conclude, we find that the microwaves and the plasma waves appear together with the discharge-current oscillations.

Finally the energy distribution of electrons reaching the cathode wall from the discharge plasma during cathode-sheath collapse has been measured. This was done with a multigrad electrostatic plasma analyzer located at the cathode wall and operating in the electron collecting regime. The measurements showed that whenever $I_a \geq 9$ A a hot Maxwellian tail appeared in the electron distribution function together with plasma waves. The temperature of these hot electrons was ~ 75 eV although the temperature of the bulk electrons was 7–8 eV, as mentioned above. The temperature of the hot electrons did not depend on the discharge current I_a while their density grew up monotonically with I_a (see Fig. 8). The maximum density of the hot electrons, at large discharge current, reached approximately 1% of the total electron

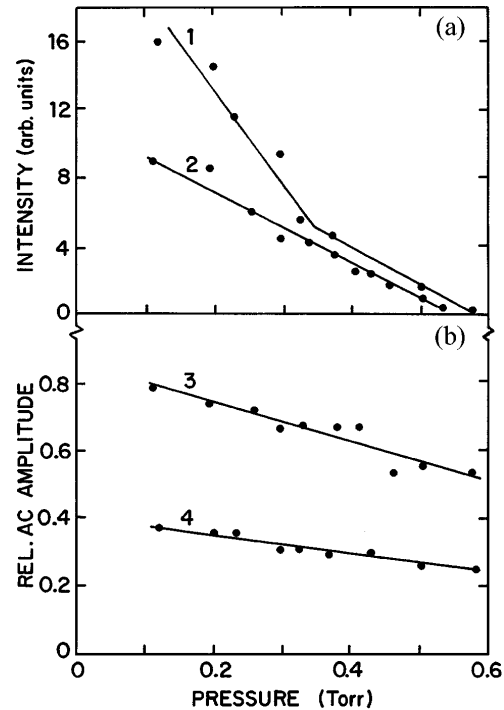


FIG. 7. (a) The microwave intensity vs pressure for $I_a = 42$ A (1) and 20 A (2). (b) The relative ac amplitude vs pressure for $I_a = 20$ A (3) and 42 A (4).

plasma density near the cathode wall. Note that the measured hot tail of the bulk electron plasma distribution is a convenient indicator for the appearance of plasma oscillations [5].

The plasma electrons reached the analyzer in periodic narrow spikes during the cathode sheath collapses. Scope traces of the electron current to the plasma analyzer are shown in Fig. 9 together with scope traces of the microwave spikes. It is clear that the peaks of the electron current from the plasma to the cathode (upper trace in Fig. 9) occurred when the cathode fall collapsed and its

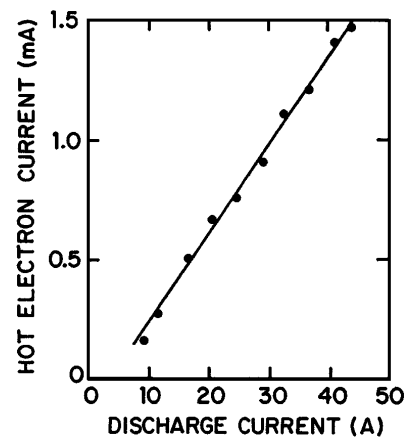


FIG. 8. Fast electron current to the electrostatic plasma analyzer vs the discharge current I_a . $P = 0.1$ Torr.

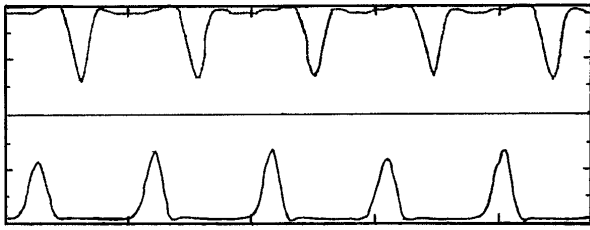


FIG. 9. Scope traces of the fast-electron current (top) and microwave radiation (bottom). Time base 40 ns/div.; $I_a = 15$ A; $P = 0.1$ Torr. Vertical scale in arbitrary units.

voltage was at minimum. Then the process of cathode-sheath reconstruction starts, characterized by growth of the sheath voltage. Electrons emitted from the cathode are accelerated into the plasma by this growing voltage. They obtain maximum energy at the moment of maximum sheath voltage. It seems reasonable to assume that this is also the time of microwave generation. As seen in Fig. 9 (lower trace), the microwave spikes indeed appear just slightly later than the middle of the period between two collapses, i.e., when the cathode fall voltage is close to its maximum.

To explain the plasma-wave generation the most probable candidate is the interaction between the beam of emitted electrons and the plasma in the vicinity of the collisionless cathode sheath. In fact, plasma waves have already been found near the collisionless sheath which surrounds a small positive probe [6]. This happens when the electron beam passes the sheath with an energy of $20-100T_e$ which in our case should be $150-750$ eV for $T_e = 7.5$ eV. In the present experiments the plasma waves do start from a current threshold of about 8–9 A which corresponds to a cathode-fall voltage of about 400 V [1], i.e., close to the middle of the above energy range where the growth rate of these waves is maximal. This maximal growth rate γ_m may be estimated as [6] $\gamma_m/\omega_e \approx 9\pi^2(n_b/n_e)(\lambda_e/d) \approx 6 \times 10^{-3} - 10 \times 10^{-3}$. Here n_b is the density of the emitted electrons, $n_b/n_e \approx 1 \times 10^{-4} - 2 \times 10^{-4}$, $\lambda_e = v_b/\omega_e$, $v_b = (2eV_c/m)^{1/2}$, e and m are, respectively, the electron charge and mass, and d is the sheath thickness. The value of d can be estimated by $d = (V_c/T_e)^{3/4}r_d$ [7], where r_d is the Debye length.

The damping of the plasma waves is $\nu/\omega_e \approx 3 \times 10^{-3}$, where ν is the electron-neutral collision frequency. The minimal value of the damping is just 2–3 times smaller than the estimated growth rate which readily explains the occurrence of the plasma waves at low gas pressure (~ 0.1 Torr) and their disappearance at higher pressure (Fig. 7). The wide frequency spectrum of these waves (Fig. 4) can be understood by the short duration of

each spike as well as by the plasma density inhomogeneity (changes in ω_e) as seen in Fig. 2. It seems reasonable that due to this inhomogeneity the plasma waves are converted to microwaves and radiated out. It becomes clear now that this kind of microwave generation is a unique property of hollow-cathode discharges because in similar plane-electrode cold-cathode discharges there are more collisions in the cathode sheath and the threshold can never be reached.

Another mechanism for microwave generation could be related with electrons orbiting in a high- Q microwave resonator [3]. However, it is not valid here because there is no thin wire in the cathode cylinder, i.e., no orbiting electrons. Also from the observed wide microwave spectrum it is clear that there is no high- Q resonator.

To conclude, we observed nanosecond pulses of microwave radiation associated with the cathode-sheath instability of a hollow-cathode discharge. During each cycle of the discharge-current oscillations the cathode sheath collapses, then it is rebuilt to its maximal voltage. At the maximal sheath voltage the beam of electrons emitted from the cathode and accelerated into the plasma creates a beam-plasma instability and plasma waves. These plasma waves are converted into radiated electromagnetic waves due to the plasma inhomogeneity. In addition, a hot electron tail is produced in the plasma electron distribution. Then the next cycle of the periodic cathode-sheath collapse starts.

This work was supported in part by the U.S. Air Force Office of Scientific Research under Grant No. AFOSR-88-0343.

-
- [1] D. Arbel, Z. Bar-Lev, J. Felsteiner, A. Rosenberg, and Ya. Z. Slutsker, Phys. Rev. Lett. **71**, 2919 (1993); Appl. Phys. Lett. **66**, 1193 (1995).
 - [2] W. Knauer, A. Fafarman, and R.L. Poeschel, Appl. Phys. Lett. **3**, 7 (1963); R.P. Babertsyan, E.S. Badalyan, G.A. Egiazaryan, and E.I. Ter-Gevorkyan, Sov. Phys. Tech. Phys. **30**, 41 (1985).
 - [3] I. Alexeff and F. Dyer, Phys. Rev. Lett. **45**, 351 (1980); I. Alexeff, Phys. Fluids **28**, 1990 (1985).
 - [4] A.A. Andronov and Yu.V. Chugunov, Sov. Phys. Usp. **18**, 343 (1975).
 - [5] Yu. Ya. Brodskii, S.I. Nechuev, Ya.Z. Slutsker, A.M. Feigin, and G.M. Fraiman, Sov. J. Plasma Phys. **15**, 688 (1989); Yu. Ya. Brodskii, V.L. Gol'tsman, S.I. Nechuev, and Ya. Z. Slutsker, Sov. Phys. Tech. Phys. **30**, 46 (1985).
 - [6] R.L. Stenzel, Phys. Rev. Lett. **60**, 704 (1988); Phys. Fluids B **1**, 2273 (1989).
 - [7] See, e.g., F.F. Chen, in *Plasma Diagnostic Techniques*, edited by R.H. Huddlestone and S.L. Leonard (Academic, New York, 1965), Chap. 4.